Hindawi
Journal of Applied Mathematics
Volume 2022, Article ID 9491308, 12 pages
https://doi.org/10.1155/2022/9491308

Research Article

Unsteady MHD Thin Film Flow of a Second-Grade Fluid past a Tilted Plate under the Impact of Thermal Radiation and Chemical Reaction

Mehari Fentahun Endalew,[1] **Masitawal Demsie Goshu**,[1] **and Yimer Chekol Tegegne**[2]

[1]*Department of Mathematics, Debre Tabor University, Debre Tabor 272, Ethiopia*
[2]*Department of Mathematics, Injibara University, Injibara 40, Ethiopia*

Correspondence should be addressed to Mehari Fentahun Endalew; mehexf@gmail.com

Received 14 February 2022; Revised 2 April 2022; Accepted 1 August 2022; Published 25 August 2022

Academic Editor: Anum Shafiq

This paper explores the impact of chemical reaction and thermal radiation on time-dependent hydromagnetic thin-film flow of a second-grade fluid across an inclined flat plate embedded in a porous medium. The thermal radiation based on the Rosseland approximation is incorporated in the energy equation. Uniform applied magnetic field and first-order homogenous chemical reaction are included in the momentum and concentration equations, respectively. The novel mathematical flow model is constructed by using a set of partial differential equations (PDEs). The PDEs are then transformed into an equivalent set of ordinary differential equations (ODEs) and solved by applying the Laplace transform method. However, the time domain solutions are obtained by using the INVLAP subroutine of MATLAB. Physical parameters influencing thin-film velocity, temperature, and concentration are illustrated graphically, while those affecting skin friction, heat, and mass transfer rates are presented in a tabular form. It is found that thin-film velocity and temperature boost with increasing values of thermal radiation, but thin-film velocity decreases with increasing values of chemical reaction and magnetic field. The current investigation is to enhance heat and mass transfer in the design of mechanical systems involving the thin film flow of second-grade fluids over an inclined flat plate after applying thermal radiation and chemical reaction.

1. Introduction

The class of fluid dynamics dealing with the interaction between electrically conducting fluids (such as saltwater, electrolytes, or molten metals) and magnetic field is known as magnetohydrodynamics (MHD). This discipline studies the interaction of the electromagnetism and fluid dynamics. MHD finds several applications in engineering and sciences such as astrophysics, geophysics, sensors, MHD power generation, and magnetic drug targeting. Obvious verifications and some applications are precisely discussed in the interesting books of Roberts [1] and Davidson and Belova [2]. An analytical study of MHD flow due to a linearly accelerating and oscillating slanted plate under the influences of thermal radiation and homogenous first-order chemical reaction is investigated in a closed form by Endalew and Nayak [3] and Endalew et al. [4]. Particularly, they have performed to investigate the effects of an inclined magnetic field, thermal radiation, and chemical reaction on time-dependent MHD flow due to inclined plate through a porous medium. McWhirter et al. [5] carried out experimental results on magnetohydrodynamics flows in a porous medium.

Second-grade fluids are a subclasses of non-Newtonian fluids in which the velocity field has a second order derivative in stress strain tensor relationship. Particularly, these fluids can be determined based on the truncation order of tensor, viz. Rivlin-Ericksen tensors in describing the Cauchy stress tensor. When the order truncation of Rivlin-Ericksen tensors becomes two, these fluids can be known as second-grade fluids. A comparative study on Newtonian and non-Newtonian base fluids is discussed by Hakeem et al. [6]. A wide range of applications of non-Newtonian fluids are gas

storage reservoirs, petroleum drilling, glaciology, the flow of cardiovascular, and undertaking the uniformity of materials in complex multiphase products such as paints, inks, and ceramic pastes. By keeping all of these significances in mind, several scholars are devoted to the investigation of second-grade fluids in different physical configurations. Among those researchers, Sarkar et al. [7] and Endalew et al. [8] studied the manner of MHD flow of second-grade fluid in a microchannel filled with a porous material. Additionally, Hayat et al. [9] and Bilal et al. [10] performed investigations on a second-grade fluid in various geometrical configurations.

Most of the aforementioned studies did not consider the mechanism of thin-film flow, which is the most important concern of the present study. Here, mathematical models are given for thin film flows on an inclined flat plate embedded in a porous medium with effects of heat and mass transfer. However, a thin film can be defined as a material layer having a thickness ranging from a fraction of a nanometer to several micrometers. The flow of fragile films whose height is substantially smaller than their length is referred to as thin-film flow (see Gul et al. [11]). As stated above, the size of the thin film is typically in the range of microns or less. Therefore, thin-film flows have applications in microchip creation, chemistry, biology, and numerous fields. Some of their applications in those areas are condensers, evaporators, thin-film reactors, distillation columns, improving fire resistance, and others. The prospects of geophysical and environmental engineering have been related to debris flows, lava, and mudslides (see Endalew and Sarkar [12]). The actual use of thin-film layers arises due to their tiny thickness, which helps in enhancing heat and mass transfer per unit volume.

Moreover, many researchers worldwide have been making considerable efforts since the past decades to investigate the flow of natural convection through porous media due to its various engineering and scientific applications. Some of these applications are heat exchangers in high heat flux, thermal energy storage, air conditioning systems, electronic equipment, sensible heat storage, and filtration process. So far, free or natural convection of heat and mass transfer through porous media have been investigated by several well-known researchers. Prasad et al. [13] studied the behavior of natural convection within a permeable medium. The model for mass and heat transfer using partial differential equations within a porous medium has been explored by Endalew and Sarkar [14]. In this research work, they have investigated important aspects of heat and mass transfer effects on MHD flow past through a porous medium. Recently, an analytical study of heat and mass transfer effects on a transient Casson fluid flow across an inclined plate is examined by Endalew [15].

Nowadays, the study of MHD convective flow problems with thermal radiation and chemical reactions has become more important in industrial technology. Thus, understanding the concept of thermal radiation and chemical reaction is the main focus of this area of work. MHD convective flow with thermal radiation and chemical reaction effects is studied by Endalew and Sarkar [16]. In this study, they conducted an analytical study of thermal radiation, and chemical reaction effect on natural convective MHD flow within porous medium. An important study on thermal radiation in nonlinear form is investigated by Saranya et al. [17] and Abdul Hakeem et al. [18]. As mentioned in this study, the consideration of nonlinear form thermal radiation utilizes to present the more general form of radiation phenomenon, and we have generated the linear form of thermal radiation in this research to investigate its effect in the considered geometrical aspect. Time-dependent convective MHD flow and heat transfer of viscous fluid through a porous surface are investigated by Alshehri et al. [19]. Radiation effect on MHD boundary layer flow with heat and mass transfer across a porous medium is discussed by Reddy et al. [20]. Moreover, Hayat et al. [21] explored the effects of a chemical reaction and thermal radiation on hydromagnetic convective flow through a curved stretching sheet.

As per our careful review of abovementioned studies, we believe that no investigation has been conducted on hydromagnetic thin-film flow of second-grade fluid over a tilted flat plate embedded through a porous medium with combined effects of mass and heat transfer including the influences of thermal radiation and first order homogeneous chemical reaction. Hence, the primary purpose of this study is to investigate the effects of thermal radiation, applied magnetic field, inclination angle of the plate, and chemical reaction on a transient MHD thin-film flow of a second-grade fluid past a porous medium across a tilted plate. Linear partial differential equations are used to express the governing equations. These equations are transformed into ordinary differential equations and solved by using the Laplace transform method. The numerical inversion is then performed using the INVLAP subroutine of MATLAB to obtain solutions in the time domain. Emerging parameters affecting the behaviors of thin film velocity, temperature, concentration, shearing stress, heat, and mass transfer rates are displayed graphically as well as in a tabular form. The investigation of MHD thin film flow of second grade fluid across an inclined plate along with thermal radiation can play a great role in manufacturing engineering procedures such as solar energy modernization, production of electric power, wire and fiber coating, paper production, and other geological problems. Moreover, thin film flow can be engineered to control the amount of light reflected or transmitted at a surface for given wavelength.

2. Basic Equations and Mathematical Foundation of the Problem

As shown in Figure 1, electrically conducting and chemically reacting MHD thin film flow of a second-grade fluid over an inclined flat plate through a porous medium is considered in this study. The thickness of the film denoted by δ on the plate is assumed to be uniform. The plate makes angle θ with the horizontal axis. Away from the plate, the temperature and concentration are given by $T_\infty{}'$ and $C_\infty{}'$, respectively. Gravity opposes the movement of the fluid and attempts to force the film to flow across the plate. A transversally uniform magnetic field is also applied to the tilted plate. At a

time $t' > 0$, the plate temperature and species concentration are raised to T'_w and C'_w, respectively, which are thereafter maintained. No-slip condition at $y' = 0$ is considered for the thin film velocity, followed by the attainment of uniform velocity at a distance δ, which is appropriate according to the thin film assumption established in Refs. [11, 12, 22, 23]. Following Refs. [11, 22, 23], the constitutive equation for the incompressible second-grade fluid is given as

$$T = -PI + \mu A_1 + \alpha_1 A_2 + \alpha_2 A_1^2. \tag{1}$$

Here, the kinematic tensors denoted by A_1 and A_2 can be expressed as follows:

$$\begin{aligned} A_1 &= (\nabla V)^T + \nabla V, \\ A_2 &= \frac{dA_1}{dt} + A_1(\nabla V)^T + (\nabla V)A_1, \end{aligned} \tag{2}$$

where d/dt is the material time derivative, V specifies the velocity, and ∇ denotes the gradient operator.

The momentum and continuity equations for the incompressible fluid can be expressed as

$$\begin{aligned} \rho \frac{DV}{Dt} &= \text{div}\,(T) + F + \rho g, \\ \text{div}\,(V) &= 0. \end{aligned} \tag{3}$$

For the uniform magnetic field, the Lorentz force is given by $F = J \times B = (0, \sigma B_o^2 u'(y,t), 0)$. Here, J specifies the density of current and B denotes the total magnetic field.

The second-grade fluid provided in Equation (1) is compatible with thermodynamics; then, the material constants should be restricted as follows (see Tan and Masuoka [22] and Dunn and Fosdick [23]):

$$\mu \geq 0, \alpha_1 \geq 0, \alpha_1 + \alpha_2 = 0. \tag{4}$$

Based on the above assumptions, equations governing MHD thin film flow of a second grade fluid are modeled as (see Refs. [11, 12, 22])

$$\begin{aligned} \frac{\partial u'}{\partial t'} = {} & \frac{\alpha_1}{\rho} \frac{\partial^3 u'}{\partial y'^2 \partial t'} + \nu \frac{\partial^2 u'}{\partial y'^2} + g \sin\theta \\ & \cdot \left[\beta \left(T' - T'_\infty \right) + \beta * \left(C' - C'_\infty \right) \right] \\ & - \left(\frac{\nu \phi'}{K} + \frac{\sigma B_o^2}{\rho} \right) u', \end{aligned} \tag{5}$$

$$\rho C_p \frac{\partial T'}{\partial t'} = \kappa \frac{\partial^2 T'}{\partial y'^2} - \frac{\partial q_r}{\partial y'}, \tag{6}$$

$$\frac{\partial C'}{\partial t'} = D \frac{\partial^2 C'}{\partial y'^2} - k'_r \left(C' - C'_\infty \right). \tag{7}$$

Equation (5) represents the momentum equation. This equation is obtained from the physical principle of the conservation law of the momentum. The first and third terms on the right-hand side of this equation show the impact of the second-grade parameter and thermal and solutal buoyancy forces including inclination angle of the plate, respectively, while the fourth term indicates the effect of the magnetic field along with porosity of the medium. The second term in equation (6) shows the influences of thermal radiation in the MHD thin film flow second-grade fluid. Moreover, the second term in equation (7) presents the impact of chemical reaction in the concentration of the second-grade fluid.

The boundary and initial conditions are as follows:

(i) At $t' = 0$,

$$u'\left(0, y'\right) = 0, C'\left(0, y'\right) = C'_\infty, T'\left(0, y'\right) = T'_\infty, \quad \text{for } 0 \leq y' \leq \delta, \tag{8}$$

(ii) At $t' > 0$,

$$\begin{aligned} & u'\left(t', 0\right) = 0, C'\left(t', 0\right) = C'_w, T'\left(t', 0\right) = T'_w, \\ & \frac{\partial u'\left(t', \delta\right)}{\partial y'} = 0, C'\left(t', \delta\right) = C'_\infty, T'\left(t', \delta\right) = T'_\infty. \end{aligned} \tag{9}$$

The radiation heat flux is expressed based on Rosseland approximation by assuming an optically thick fluid (see Siegel [24] and Hussanan et al. [25]) and can be written as

$$q_r = -\frac{4\varepsilon \partial T'^4}{c * \partial y'}. \tag{10}$$

In the above equation, $c*$ and ε symbolize the absorption and Stefan-Boltzmann constants, respectively. The temperature variation throughout the problem is assumed to be very small. Therefore, the temperature T'^4 will be described as in terms of fluid temperature distribution in the system. Applying the expansion of Taylor series in T'^4 about T'_∞ and keeping away from its higher order, we have found the following equation:

$$T'^4 \cong 4T'^3_\infty T' - 3T'_\infty 4. \tag{11}$$

By putting equations (10) and (11) into equation (6), the temperature equation reduces as follows:

$$\rho C_p \frac{\partial T'}{\partial t'} = \kappa \left(1 + \frac{16 \varepsilon T'^3_\infty}{3c * \kappa} \right) \frac{\partial^2 T'}{\partial y'^2}. \tag{12}$$

Inserting the following dimensionless quantities into equations (5) to (9):

$$\left.\begin{aligned} &y=\frac{y'}{\delta}, u=\frac{u'\delta}{\nu}, t=\frac{t'\nu}{\delta^2}, \mathrm{Sc}=\frac{\nu}{D}, T=\frac{T'-T_\infty{}'}{T_w'-T_\infty{}'}, C=\frac{C'-C_\infty{}'}{C_w'-C_\infty{}'},\\ &\mathrm{Gc}=\frac{g\beta*\left(C_w'-C_\infty{}'\right)\delta^3}{\nu^2}, \mathrm{Gr}=\frac{g\beta\left(T_w'-T_\infty{}'\right)\delta^3}{\nu^2}, \mathrm{Pr}=\frac{\mu C_p}{\kappa},\\ &\alpha=\frac{\alpha_1}{\rho\delta^2}, M=\frac{\sigma B_o^2\delta^2}{\rho\nu}, R=\frac{16\varepsilon T_\infty{}'3}{c*\kappa}, k_r=\frac{\delta^2 k_r'}{\nu}, \phi=\frac{\delta^2\phi'}{K}, \end{aligned}\right\} \tag{13}$$

we obtain the dimensionless equations as

$$\frac{\partial u}{\partial t}=\frac{\partial^2 u}{\partial y^2}+\alpha\frac{\partial^3 u}{\partial y^2\partial t}-(\phi+M)u+[\mathrm{Gr}T+\mathrm{Gc}C]\sin\theta, \tag{14}$$

$$\frac{\partial T}{\partial t}=\left(\frac{1+R}{\mathrm{Pr}}\right)\frac{\partial^2 T}{\partial y^2}, \tag{15}$$

$$\frac{\partial C}{\partial t}=\frac{1}{Sc}\frac{\partial^2 C}{\partial y^2}-k_r C. \tag{16}$$

The nondimensional initial and boundary conditions are

$$t=0: u(y,0)=C(y,0)=T(y,0)=0, \quad \text{for } 0\le y\le 1, \tag{17a}$$

$$t>0: \begin{cases} u(0,t)=0, C(0,t)=T(0,t)=1,\\ \dfrac{\partial u(1,t)}{\partial y}=C(1,t)=T(1,t)=0. \end{cases} \tag{17b}$$

3. Solution Technique

Using the Laplace transform technique, the governing partial differential equations (14), (15) and (16) along with their boundary conditions (17b) are reduced into an equivalent set of ordinary differential equations by applying initial conditions (17a). Hence, the transformed ordinary differential equations (ODEs) are obtained as

$$\begin{aligned} \frac{d^2\tilde{u}(y,s)}{dy^2}-\left[\zeta\tilde{u}(y,s)+\eta\tilde{T}(y,s)+\psi\tilde{C}(y,s)\right]&=0,\\ \frac{d^2\tilde{T}(y,s)}{dy^2}-sPe\tilde{T}(y,s)&=0,\\ \frac{d^2\tilde{C}(y,s)}{dy^2}-[s\mathrm{Sc}+\mathrm{Sc}k_r]\tilde{C}(y,s)&=0, \end{aligned} \tag{18}$$

where $\zeta=(s+\phi+M)/(1+\alpha s)$, $\eta=-\mathrm{Gr}\sin\theta/(1+\alpha s)$, $\psi=-\mathrm{Gc}\sin\theta/(1+\alpha s)$, $Pe=\mathrm{Pr}/(1+R)$.

Moreover, the transformed boundary conditions of the flow model are given as

$$\begin{aligned} &\tilde{u}(y,s)=0, \tilde{T}(y,s)=\frac{1}{s}, \tilde{C}(y,s)=\frac{1}{s} \text{ at } y=0,\\ &\frac{d\tilde{u}(y,s)}{dy}=0, \tilde{T}(y,s)=0, \tilde{C}(y,s)=0 \text{ at } y=1. \end{aligned} \tag{19}$$

From the above equations, the transformed velocity, temperature, and concentration fields in Laplace domain are denoted by $\tilde{u}(y,s)$, $\tilde{T}(y,s)$ and $\tilde{C}(y,s)$, respectively.

Then, the solutions for velocity, temperature, and concentration can be provided as

$$\begin{aligned} \tilde{u}(y,s)=c_1e^{-y\sqrt{\zeta}}+c_2e^{y\sqrt{\zeta}}+c_3\sinh\sqrt{sPe}(1-y)\\ +c_4\sinh\sqrt{s\mathrm{Sc}+\mathrm{Sc}k_r}(1-y), \end{aligned} \tag{20}$$

$$\tilde{T}(y,s)=\frac{\sinh\sqrt{sPe}(1-y)}{(s)\sinh\sqrt{sPe}}, \tag{21}$$

$$\tilde{C}(y,s)=\frac{\sinh\sqrt{s\mathrm{Sc}+\mathrm{Sc}k_r}(1-y)}{(s)\sinh\sqrt{s\mathrm{Sc}+\mathrm{Sc}k_r}}. \tag{22}$$

The coefficients are defined as follows:

$$\begin{aligned} c_1=&\frac{-\eta}{2s(sPe-\zeta)\cosh\sqrt{\zeta}}\left[\frac{\sqrt{sPe}}{\sqrt{\zeta}\sinh\sqrt{sPe}}+e^{\sqrt{\zeta}}\right]\\ &-\frac{\psi}{2s(s\mathrm{Sc}+\mathrm{Sc}k_r-\zeta)\cosh\sqrt{\zeta}}\left[\frac{\sqrt{s\mathrm{Sc}+\mathrm{Sc}k_r}}{\sqrt{\zeta}\sinh\sqrt{s\mathrm{Sc}+\mathrm{Sc}k_r}}+e^{\sqrt{\zeta}}\right],\\ c_2=&\frac{\eta}{2s(sPe-\zeta)\cosh\sqrt{\zeta}}\left[\frac{\sqrt{sPe}}{\sqrt{\zeta}\sinh\sqrt{sPe}}-e^{-\sqrt{\zeta}}\right]\\ &+\frac{\psi}{2s(s\mathrm{Sc}+\mathrm{Sc}k_r-\zeta)\cosh\sqrt{\zeta}}\left[\frac{\sqrt{s\mathrm{Sc}+\mathrm{Sc}k_r}}{\sqrt{\zeta}\sinh\sqrt{s\mathrm{Sc}+\mathrm{Sc}k_r}}-e^{-\sqrt{\zeta}}\right],\\ c_3=&\frac{\eta}{s(sPe-\zeta)\sinh\sqrt{sPe}}, c_4=\frac{\psi}{s(s\mathrm{Sc}+\mathrm{Sc}k_r-\zeta)\sinh\sqrt{s\mathrm{Sc}+\mathrm{Sc}k_r}}. \end{aligned} \tag{23}$$

However, it is difficult to invert equations (20)–(22) to achieve the desired solutions to the original problems in order to obtain the velocity, temperature, and concentration in the time domain. To avoid this difficulty, we employed INVLAP subroutine of MATLAB [26], which is proposed by De Hoog et al. [27]. Mainly, it is proposed based on accelerating the convergence of Fourier series obtained from the inversion integral using the trapezoidal rule. The function INVLAP offers a simple, effective and convincingly accurate way to achieve the results. It solves even fractional problems and invert functions containing irrational, rational, and transcendental expressions with high accuracy and low computational errors.

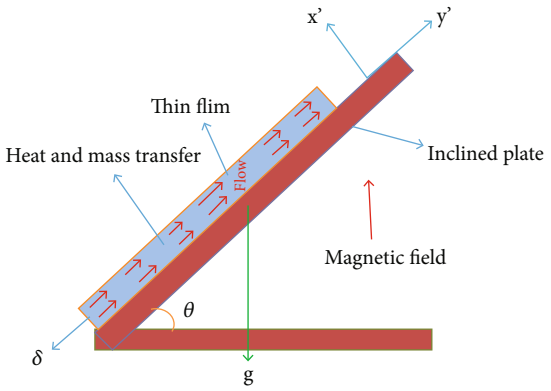

Figure 1: Schematic diagram of the thin film flow.

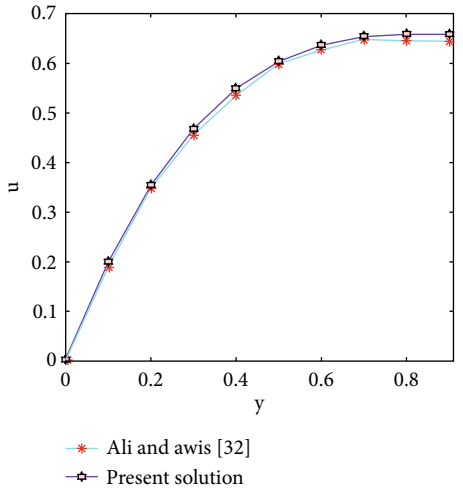

Figure 2: Validity of results.

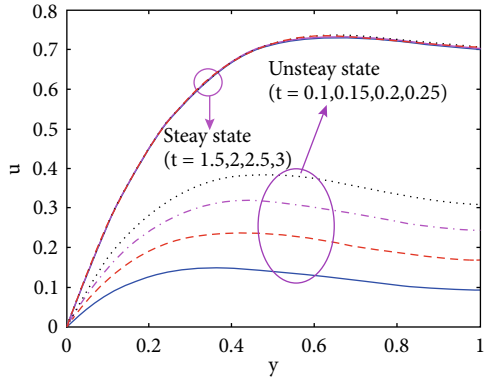

Figure 3: Thin film velocity profiles for various t.

4. Skin Friction and Heat and Mass Transfer Rates

Physical interests including skin friction, mass transfer rate, and heat transfer rate play a vital role in the study of viscous fluid dynamics. They are derived from solutions of velocity, temperature, and concentration as clearly stated below.

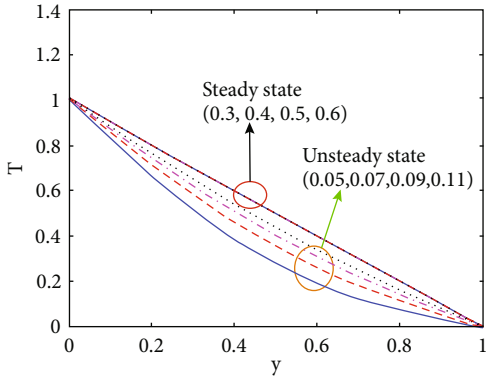

Figure 4: Temperature profiles for various t.

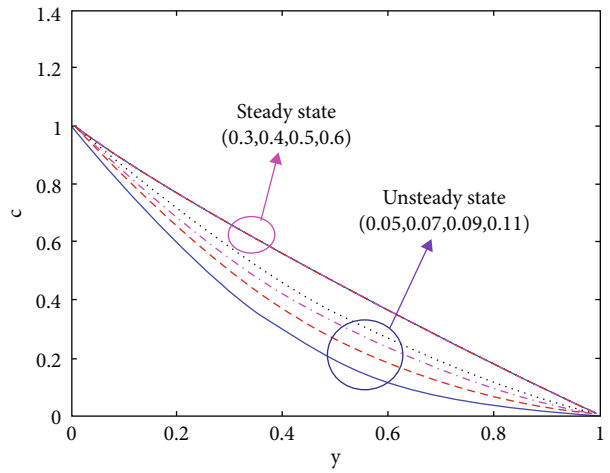

Figure 5: Concentration profiles for various t.

4.1. Skin Friction. It is an important dimensionless physical quantity in boundary layer flows and can be computed by putting $y = 0$ in equation (20). Then, it can be written as

$$\tau_0 = \left.\frac{\partial \bar{u}(y,s)}{\partial y}\right|_{y=0} = \sqrt{\zeta}(-c_1 + c_2) - c_3\sqrt{sPe}\cosh\sqrt{sPe} - c_4\sqrt{sSc + Sck_r}\cosh\sqrt{sSc + Sck_r}. \quad (24)$$

4.2. Heat Transfer Rate. The amount of heat that could be transferred per unit time in some materials is known as heat transfer rate or Nusselt number. This physical entity can be computed at the end of the surfaces or walls ($y = 0$ and $y = 1$). Its solution is obtained from equation (21) and expressed as follows.

$$\mathrm{Nu}_0 = \left.\frac{\partial \tilde{T}(y,s)}{\partial y}\right|_{y=0} = -\frac{\sqrt{sPe}\cosh\sqrt{sPe}}{(s)\sinh\sqrt{sP_e}},$$
$$\mathrm{Nu}_1 = \left.\frac{\partial \tilde{T}(y,s)}{\partial y}\right|_{y=1} = \frac{-\sqrt{sPe}}{(s)\sinh\sqrt{sPe}}. \quad (25)$$

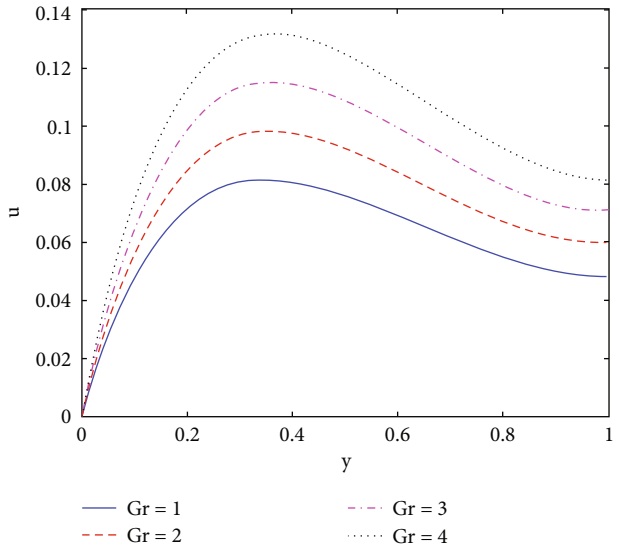

Figure 6: Thin film velocity profiles for various Gr.

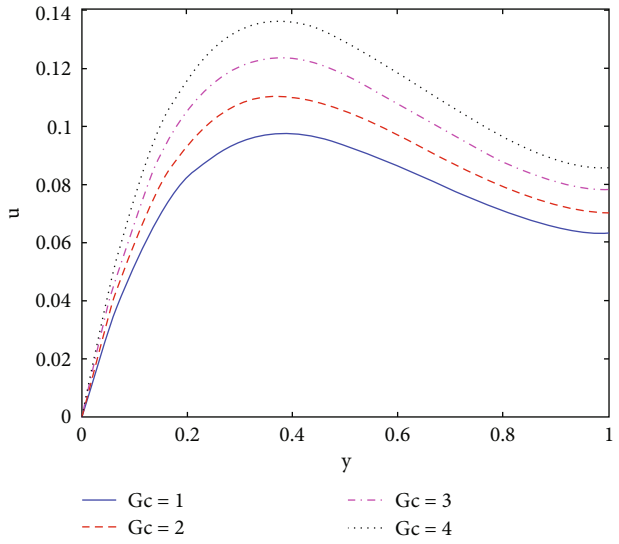

Figure 7: Thin film velocity profiles for various Gc.

4.3. Mass Transfer Rate. The mass transfer rate, often known as the Sherwood number, is a dimensionless quantity that investigates the mass transfer rate at $y = 0$ and $y = 1$. Its solution is computed from equation (22) and written as

$$\mathrm{Sh}_0 = \left.\frac{\partial \tilde{C}(y,s)}{\partial y}\right|_{y=0} = -\frac{\sqrt{s\mathrm{Sc} + \mathrm{Sc}k_r}\,\cosh\sqrt{s\mathrm{Sc} + \mathrm{Sc}k_r}}{(s)\,\sinh\sqrt{s\mathrm{Sc} + \mathrm{Sc}k_r}},$$

$$\mathrm{Sh}_1 = \left.\frac{\partial \tilde{C}(y,s)}{\partial y}\right|_{y=1} = \frac{-\sqrt{s\mathrm{Sc} + \mathrm{Sc}k_r}}{(s)\,\sinh\sqrt{s\mathrm{Sc} + \mathrm{Sc}k_r}}. \tag{26}$$

The time domain solutions for skin friction, heat, and mass transfer rates are obtained by using INVLAP-routine of MATLAB as well.

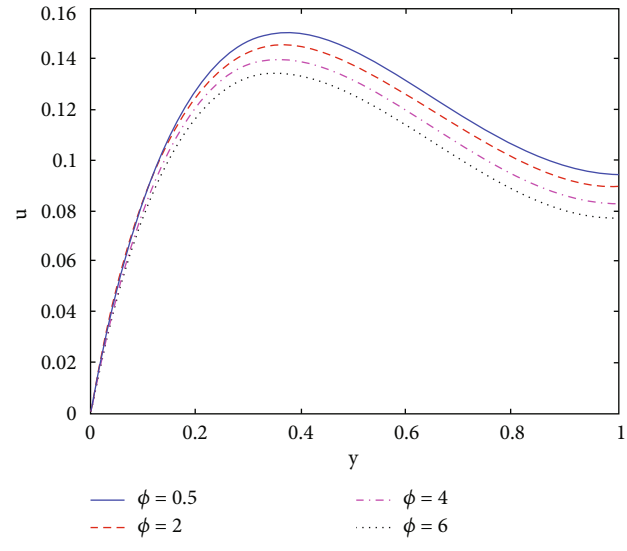

Figure 8: Thin film velocity profiles for various ϕ.

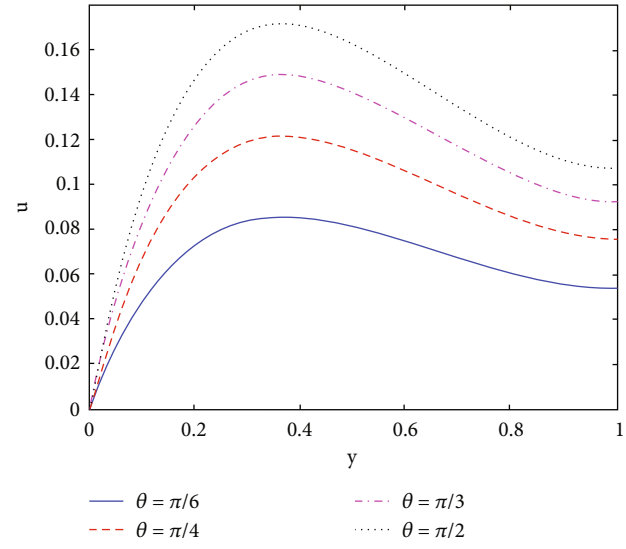

Figure 9: Thin film velocity profiles for various θ.

The present result has been authenticated with previously published articles of Ali and Awais [28]. The comparison technique has been done by extracting points corresponding to the parameter values $\phi = \alpha = t = 0.1$ in Figure 2 of Ali and Awais [28]. Then, avoiding the energy and concentration equation along with their boundary conditions and making $M = 0$, we obtained an excellent confirmation of the results as shown in Figure 3.

5. Results and Discussion

For the purpose of discussion, the influences of thermal radiation and chemical reaction on an unsteady hydromagnetic thin film flow of a second-grade fluid past through a tilted porous plate have been carried out. Graphical representation of emerging physical parameters affecting the behaviors of thin-film velocity, temperature, and concentration has been

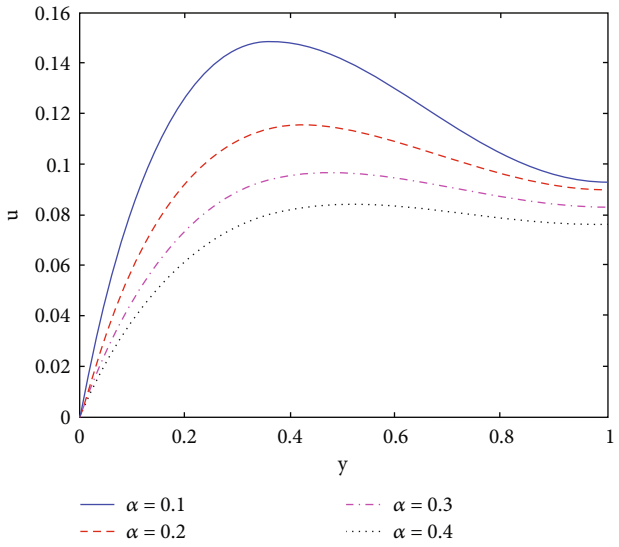

Figure 10: Thin film velocity profiles for various α.

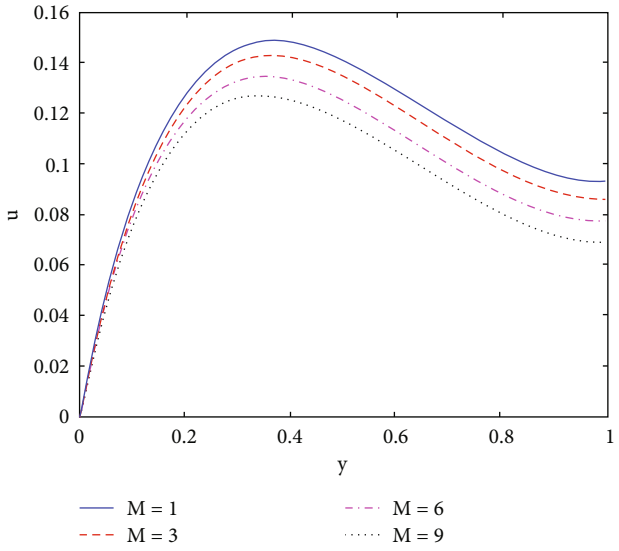

Figure 11: Thin film velocity profiles for various M.

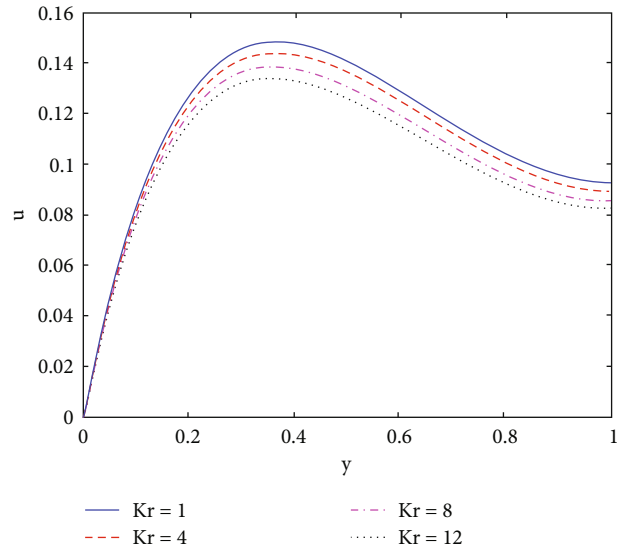

Figure 12: Thin film velocity profiles for various Kr.

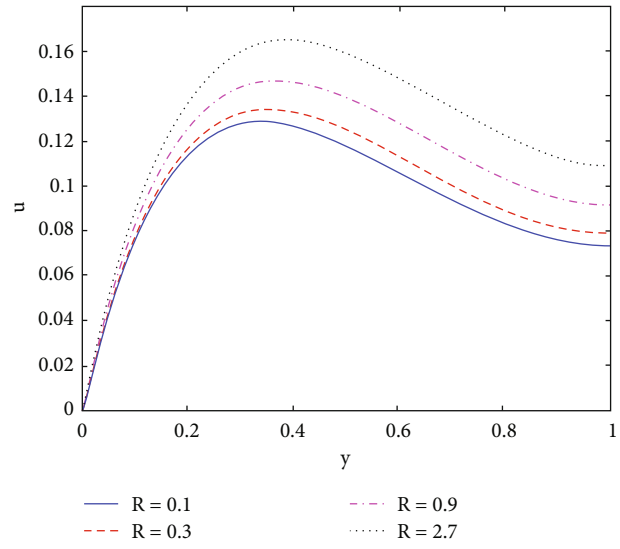

Figure 13: Thin film velocity profiles for various R.

demonstrated in Figures 3–19. Furthermore, the surface shearing stress, temperature gradient, and concentration gradient at the surface are recorded in a tabular form as indicated in Tables 1 and 2. We have taken arbitrary positive values for all physical parameters to examine their impacts on thin-film flow behaviors. Therefore, such values are assigned as $\mathrm{Sc} = 0.6$, $\mathrm{Pr} = 0.71$, $\alpha = 0.1$, $kr = M = \phi = R = 1$, $\theta = \pi/3$, $\mathrm{Gr} = 5 = \mathrm{Gc}$, and $t = 0.1$. Or else, it should be mentioned.

From the boundary conditions given in (17b), fluid velocity at $y = 0$ is zero and its value at $y = 1$ becomes any constant number for increasing values of time. Furthermore, at $y = 0$ temperature and concentration become one and their values at $y = 1$ are zero for any time. Therefore, the boundary conditions of the governing equations are satisfied as indicated in Figures 3–5. In addition, the influences of time variations along with thin-film velocity field, temperature, and concentration gradients are illustrated in Figures 3–5. Here, all fluid behaviors such as velocity, temperature, and concentration amplify upon augmentation of time.

Most significantly, our emphasis on unsteady to steady analysis is clearly illustrated by these figures. Therefore, the result of velocity changes or becomes unsteady at $t = 0.1$, 0.15, 0.2, 0.25. However, it reaches steady state at $t = 1.5$. Moreover, both fluid temperature and concentration become unsteady state at $t = 0.05, 0.07, 0.09, 0.11$ and attain steady state at $t = 0.3$.

Physically speaking, thermal Grashof and solutal Grashof numbers are dimensionless quantities that describe the free or natural convection mechanisms in a flow system. Arbitrary positive values are chosen for these quantities to

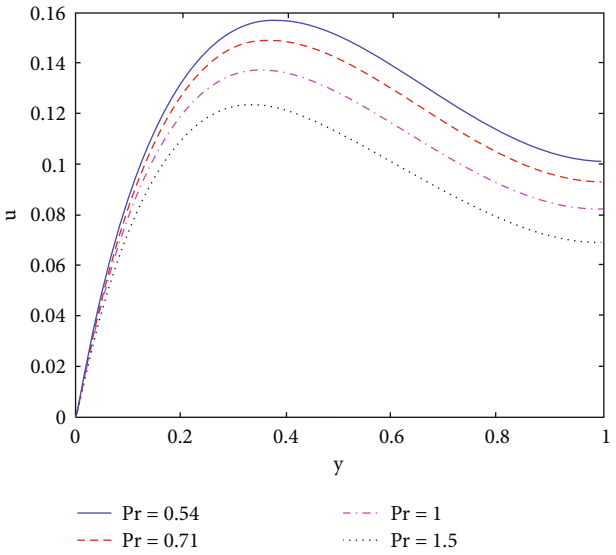

Figure 14: Thin film velocity profiles for various Pr.

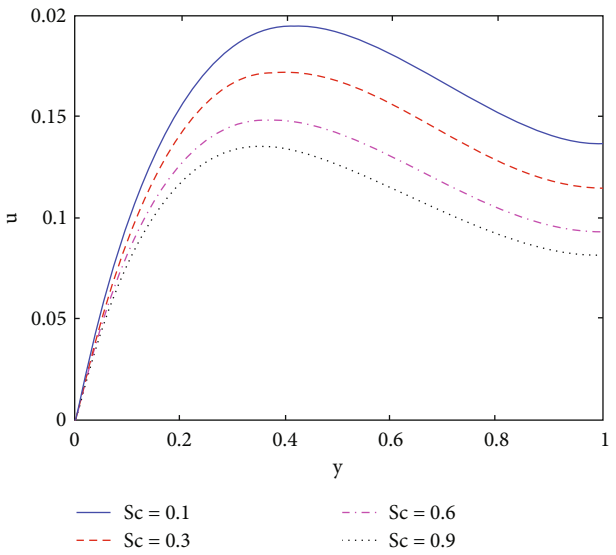

Figure 15: Thin film velocity profiles for various Sc.

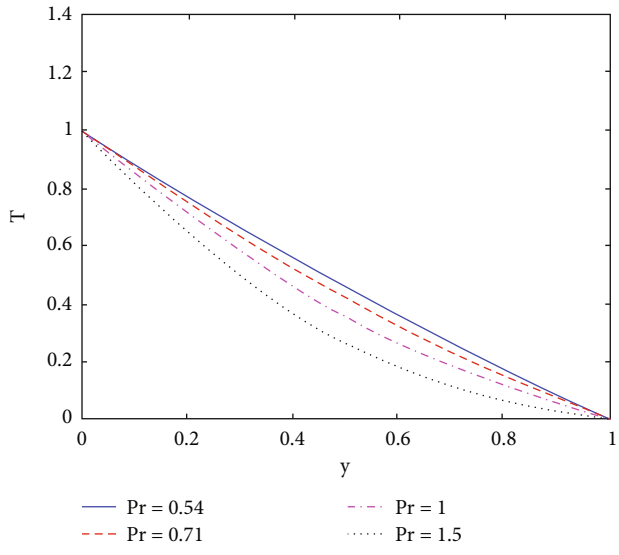

Figure 16: Temperature profiles for various Pr.

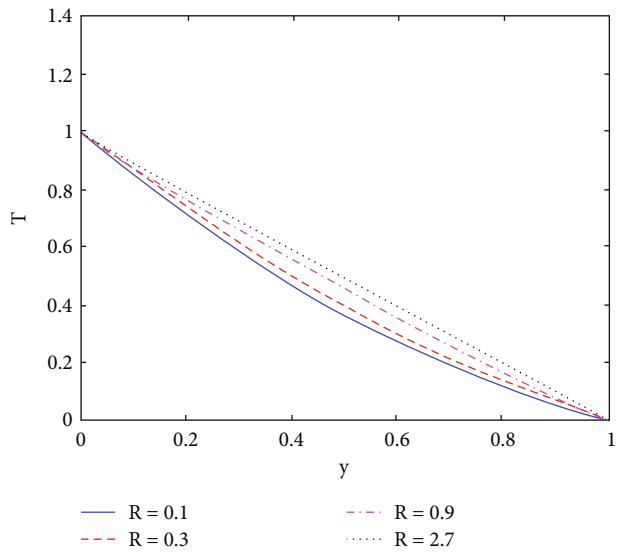

Figure 17: Temperature profiles for various R.

illustrate fluid flow characteristics. The assumptions of positive values for these physical quantities tell us the second-grade fluid is heated or the skewed plate is cooled. That means heat flows away from the inclined plate into the boundary region of the system. Therefore, the fluid motion is caused by the gravity-driven force viz. buoyancy force. Owing to this, the thin film velocity boosts with increasing values of both Grashof numbers, as publicized in Figures 6 and 7.

A porosity is a measure of the empty space in the medium. Furthermore, it is a volume fraction of the vacant space over the total volume. Physically speaking, a high porosity in the permeable medium causes the enlargement of the thin film thickness or the permeability reduction at the edge of the medium. This is due to its inverse proportionality to the permeability of the medium. In this line, an increment of porosity causes the reduction in the thin-film flow, as indicated in Figure 8. Additionally, as the porosity parameter increases, the medium's void or empty space increases and that leads to the declaration of the thin film flow.

The numerical variations of the inclination angle of the plate that ranges from $\pi/6$ to $\pi/2$ are indicated in Figure 9. From the physics concept, one certainly can understand that as the plate closes to the normal axis, the thin film flow will be accelerating, and then, it is a fact that its velocity increases.

The influence of a second-grade entity on time-dependent thin-film velocity is captured in Figure 10. It is evident to say that the thin film velocity decelerates with

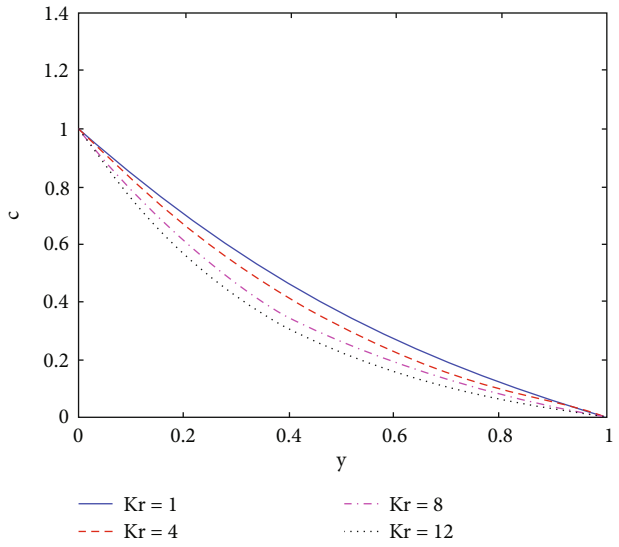

Figure 18: Concentration profiles for various Kr.

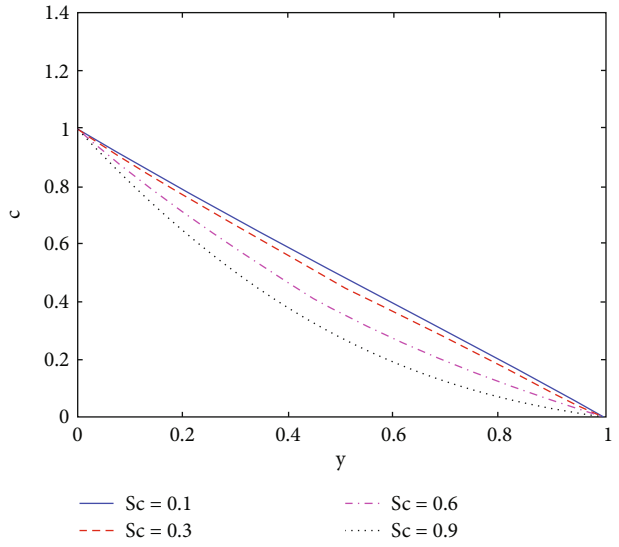

Figure 19: Concentration profiles for various Sc.

the increment of the second-grade parameter of the fluid. This is due to the existence of a viscous force that dominates the flow in the system. Therefore, an increase of the second grade parameter yields an extra thin film thickness by its nature. Therefore, the reduction of thin-film flow as pointed out in Figure 10 is caused by the increment of the second-grade parameter.

This investigation deals with MHD thin film flow due to the inclined plate with uniform thin film thickness through porous medium. As we have tried to mention in the introduction section, MHD plays a significant role in the application of various fields. As it can be noted, the magnetic field which is directly related to the viscous force viz. Lorentz force influences the thin film flow in its regime. This means, as the magnetic field strength boosts in the flow system, the thin film flow of second grade fluid reduces. Therefore, as the estimation values of the magnetic field enlarge, then, thin film velocity declines, as shown in Figure 11.

Table 1: Values of skin friction for different physical entities.

Sc	R	k_r	M	Pr	Gr	Gc	α	ϕ	θ	t	τ_0
0.6											0.6372
0.7											0.5811
	1										1.1256
	2										1.1336
		1									1.1256
		2									1.1036
			1								1.1256
			2								1.1505
				0.71							0.6372
				1							0.6323
					5						0.9036
					6						0.9702
						5					3.1860
						6					3.7566
							0.1				3.1860
							0.2				1.4827
								1			3.2493
								2			3.3211
									$\pi/3$		1.1256
									$\pi/2$		1.2997
										0.1	1.1256
										0.2	2.9684

The effects of chemical reaction on thin-film velocity and concentration fields are illustrated in Figures 12 and 18. Both figures show that as chemical reaction increases, thin-film velocity and concentration field decrease. In addition, Figure 13 shows that the thin-film velocity rises with an increment of thermal radiation. Furthermore, Figure 17 depicts the influence of the thermal radiation on the temperature distribution, and it can be seen that as thermal radiation grows, the temperature field increases as well.

From the physical point of view, Prandtl number is the ratio of frictional/viscous force to the thermal diffusion. Likewise, Schmidt number is the ratio of frictional/viscous force to the mass diffusion. Therefore, Prandtl and Schmidt numbers are directly proportional to viscous force and have opposite relationships with the thermal and mass diffusions, respectively. It is worth noting that viscous forces, by their very nature, constantly oppose fluid motion. Due to the reciprocal relationships with heat and mass diffusions, fluid temperature and concentration diminish with increase of Prandtl number and Schmidt numbers as shown in Figures 16 and 19.

Thin-film velocity decreases with larger Prandtl and Schmidt numbers estimations, as shown in Figures 14 and 15.

Finally, we can conclude that the fluid velocity, temperature, and concentration field diminish with the augmentation of both Prandtl and Schmidt numbers.

Table 2: Values of Nusselt and Sherwood numbers for different physical entities.

R	Pr	k_r	Sc	t	$-\mathrm{Nu}_0$	$-\mathrm{Nu}_1$	$-\mathrm{Sh}_0$	$-\mathrm{Sh}_1$
1					1.1241	0.8760		
2					1.0309	0.9691		
	0.71				1.1241	0.8760		
	1				1.2786	0.7229		
		1					1.5242	0.5798
		2					1.6553	0.5452
			0.6				1.5242	0.5798
			0.7				1.6420	0.4859
				0.1	1.1241	0.8760	1.5242	0.5798
				0.2	1.0077	0.9923	1.2499	0.8491

The impacts of several emerging physical factors on local skin friction are explored in Table 1. Skin friction increases as physical parameters such as thermal radiation, magnetic field, thermal and solutal Grashof numbers, porosity, plate inclination angle, second grade parameter, and time increase, but now it lowers as Prandtl number, Schmidt number, and chemical reaction expand.

Table 2 shows the influences of different parameters on heat and mass transfer rates at $y = 0$ and $y = 1$. Thus, at $y = 0$, the magnitude of Nusselt number increases with the increase of Prandtl number and diminishes with the increase of thermal radiation and time. However, the opposite effect is confirmed at . That is, at $y = 1$, the magnitude of Nusselt number increases as thermal radiation and time increase and decrease with the increase of Prandtl number. This table explores also the effects of Schmidt number, chemical reaction parameter, and time on Sherwood number. Here, as chemical reaction increases, the magnitude of Sherwood number increases at $y = 0$ and decreases at $y = 1$. However, when Schmidt number increases, the Sherwood number in magnitude increases at and decreases at $y = 1$, whereas as time increases, the magnitude of Sherwood number decreases at $y = 0$ and increases at $y = 1$.

6. Conclusion

In this research work, the influence of thermal radiation and chemical reaction on the time-dependent hydromagnetic thin-film flow of a second grade fluid over an inclined plate within a porous medium has been scrutinized. The governing differential equations are solved by applying Laplace transform methods, and their numerical inversions are carried out by using INVLAP subroutine of MATLAB. The current result has been compared with existing article and an excellent conformation is obtained. The important findings are noted as follows:

(i) Velocity field increases with the increase of the thermal and solutal Grashof numbers. When thermal and solutal Grashof numbers increase, the buoyant force dominates the thin film flow in the provided region. Due to this, the increase of fluid velocity is captured upon larger thermal and solutal Grashof numbers

(ii) With the increase of magnetic field, second grade parameter, and porosity, the fluid velocity diminishes. When magnetic strength becomes high, the Lorentz force which resists the fluid flow dominates the flow system. Therefore, high magnetic strength leads to resist the fluid motion. An increase of second-grade parameter causes the dominant viscous force in the flow region. This viscous force causes reduction on the fluid velocity. Moreover, porosity of the medium is inversely proportional to the permeability. This physical interpretation causes the reduction in the thin film velocity

(iii) Temperature and thermal boundary layer thickness decrease with the increase of Prandtl number. Physically speaking, it is legitimate in light of the Prandtl number which is inversely proportional to the thermal diffusion. Thus, this fact leads to reduction on fluid temperature and its boundary layer thickness

(iv) Temperature and thickness of the thermal boundary layer increase with the increase of thermal radiation. It is obvious that thermal radiation is function of temperature by its physical nature. Therefore, thermal radiation increases both temperature and its boundary layer thickness enhances

(v) Concentration and solutal boundary layer thickness diminish with the augmentation of Schmidt number and chemical reaction parameters. Schmidt number is inversely proportional to the mass diffusion by its physical elucidation. Therefore, concentration diminish upon Schmidt number increases. Additionally, chemical reaction is the process of changing the form substances to another form. Due to this, as conversion process rate increases, the concentration of the fluid becomes less

Nomenclature

u': Dimensional velocity (m/s)
g: Gravitational acceleration ($\mathrm{m/s^2}$)
K: Permeability of medium ($\mathrm{m^2}$)
B_o: Applied magnetic field ($T = \mathrm{kg/As^2}$)
C_p: Specific heat capacity (J/kgK)
T': Dimensional fluid temperature (K)
C': Dimensional fluid concentration ($\mathrm{Kmol/m^3}$)
D: Molecular diffusivity ($\mathrm{m^2/s}$)
q_r: Radiative heat flux ($\mathrm{W/m^2}$)
k_r': Chemical reaction (1/s)
t': Dimensional time (s)
u: Nondimensional velocity
M: Magnetic field
R: Thermal radiation
Gc: Solutal Grashof number
Gr: Thermal Grashof number

Sc: Schmidt number
I: Identity tensor
P: Hydrostatic pressure
T: Dimensionless temperature
C: Dimensionless concentration
t: Dimensionless time
Pr: Prandtl number
k_r: Dimensionless chemical reaction
Nu_0: Nusselt numbers at $y = 0$
Nu_1: Nusselt numbers at $y = 1$
Sh_0: Sherwood numbers at $y = 0$
Sh_1: Sherwood numbers at $y = 1$.

Greek symbols

ν: Kinematic viscosity (m^2/s)
σ: Electrical conductivity ($S/m = s^3A^2/kgm^3$)
κ: Thermal conductivity (W/mK)
ϕ: Porosity of the medium
ρ: Density of the fluid (kg/m^3)
β: Volumetric heat expansion (1/K)
$\beta*$: Volumetric mass expansion (m^3/kg)
μ: Dynamic viscosity (kg/ms)
α_1, α_2: Moduli of normal stress
δ: Thickness of thin film (m)
α: Second-grade parameter
τ_0: Skin friction at $y = 0$.

Data Availability

The data used to support the findings of this study are included within the article. The data generated using MATLAB code are already presented in tables and figures and are included in the results and discussion section of the manuscript.

Conflicts of Interest

The authors declare that they have no conflicts of interest.

References

[1] P. H. Roberts, *An Introduction to Magnetohydrodynamics*, Longmans London, 1967.

[2] P. A. Davidson and E. V. Belova, "An introduction to magnetohydrodynamics," *American Association of Physics Teachers*, vol. 70, no. 7, p. 781, 2002.

[3] M. F. Endalew and A. Nayak, "Thermal radiation and inclined magnetic field effects on MHD flow past a linearly accelerated inclined plate in a porous medium with variable temperature," *Heat Transfer-Asian Research*, vol. 48, no. 1, pp. 42–61, 2019.

[4] M. F. Endalew, A. Nayak, and S. Sarkar, "FLOW past an oscillating slanted plate under the effects of inclined magnetic field, radiation, chemical REACTION, and TIME-VARYING temperature and concentration," *International Journal of Fluid Mechanics Research*, vol. 47, no. 3, pp. 247–261, 2020.

[5] J. D. McWhirter, M. E. Crawford, and D. E. Klein, "Magneto-hydrodynamic flows in porous media II: experimental results," *Fusion Technology*, vol. 34, no. 3P1, pp. 187–197, 1998.

[6] A. A. Hakeem, S. Saranya, and B. Ganga, "Comparative study on Newtonian/non-Newtonian base fluids with magnetic/non- magnetic nanoparticles over a flat plate with uniform heat flux," *Journal of Molecular Liquids*, vol. 230, pp. 445–452, 2017.

[7] S. Sarkar, M. F. Endalew, and O. D. Makinde, "Study of MHD second grade flow through a porous microchannel under the dual-phase-lag heat and mass transfer model," *Journal of Applied and Computational Mechanics*, vol. 5, no. 4, pp. 763–778, 2019.

[8] M. F. Endalew, S. Sarkar, G. S. Seth, and O. D. Makinde, "Dual-phase-lag heat transfer model in hydromagnetic second grade flow through a microchannel filled with porous material: a time-bound analysis," *Revue des Composites et des Materiaux Avances*, vol. 28, no. 2, pp. 173–194, 2018.

[9] T. Hayat, N. Ahmed, M. Sajid, and S. Asghar, "On the MHD flow of a second grade fluid in a porous channel," *Computers & Mathematics with Applications*, vol. 54, no. 3, pp. 407–414, 2007.

[10] S. Bilal, A. H. Majeed, R. Mahmood, I. Khan, A. H. Seikh, and E. S. Sherif, "Heat and mass transfer in hydromagnetic second-grade fluid past a porous inclined cylinder under the effects of thermal dissipation, diffusion and radiative heat flux," *Energies*, vol. 13, no. 1, p. 278, 2020.

[11] T. Gul, A. S. Khan, S. Islam et al., "Heat transfer investigation of the unsteady thin film flow of Williamson fluid past an inclined and oscillating moving plate," *Applied Sciences*, vol. 7, no. 4, p. 369, 2017.

[12] M. F. Endalew and S. Sarkar, "Capturing the transient features of double diffusive thin film flow of a second grade fluid through a porous medium," *International Journal of Applied and Computational Mathematics*, vol. 5, no. 6, pp. 1–9, 2019.

[13] V. F. Prasad, F. A. Kulacki, and M. Keyhani, "Natural convection in porous media," *Journal of Fluid Mechanics*, vol. 150, pp. 89–119, 1985.

[14] M. F. Endalew and S. Sarkar, "Temporal analysis of dual phase-lag double-diffusive MHD flow within a porous microchannel with chemical reaction," *Heat Transfer—Asian Research*, vol. 48, no. 4, pp. 1292–1317, 2019.

[15] M. F. Endalew, "Analytical study of heat and mass transfer effects on unsteady Casson fluid flow over an oscillating plate with thermal and solutal boundary conditions," *Heat Transfer*, vol. 50, no. 6, pp. 6285–6299, 2021.

[16] M. F. Endalew and S. Sarkar, "Incidences of aligned magnetic field on unsteady MHD flow past a parabolic accelerated inclined plate in a porous medium," *Heat Transfer*, vol. 50, no. 6, pp. 5865–5884, 2021.

[17] S. Saranya, P. Ragupathi, B. Ganga, R. P. Sharma, and A. A. Hakeem, "Non-linear radiation effects on magnetic/non-magnetic nanoparticles with different base fluids over a flat plate," *Advanced Powder Technology*, vol. 29, no. 9, pp. 1977–1990, 2018.

[18] A. K. Abdul Hakeem, P. Ragupathi, S. Saranya, and B. Ganga, "Three dimensional non-linear radiative nanofluid flow over a Riga plate," *Journal of Applied and Computational Mechanics*, vol. 6, no. 4, pp. 1012–1029, 2020.

[19] N. A. Alshehri, A. Abidi, M. R. Khan et al., "Unsteady convective MHD flow and heat transfer of a viscous nanofluid across a porous stretching/shrinking surface: existence of multiple solutions," *Crystals*, vol. 11, no. 11, p. 1359, 2021.

[20] Y. D. Reddy, F. Mebarek-Oudina, B. S. Goud, and A. I. Ismail, "Radiation, velocity and thermal slips effect toward MHD boundary layer flow through heat and mass transport of Williamson nanofluid with porous medium," *Arabian Journal for Science and Engineering*, pp. 1–5, 2022.

[21] T. Hayat, M. Rashid, M. Imtiaz, and A. Alsaedi, "MHD convective flow due to a curved surface with thermal radiation and chemical reaction," *Journal of Molecular Liquids*, vol. 225, pp. 482–489, 2017.

[22] W. Tan and T. Masuoka, "Stokes' first problem for a second grade fluid in a porous half-space with heated boundary," *International Journal of Non-Linear Mechanics*, vol. 40, no. 4, pp. 515–522, 2005.

[23] J. E. Dunn and R. L. Fosdick, "Thermodynamics, stability, and boundedness of fluids of complexity 2 and fluids of second grade," *Archive for Rational Mechanics and Analysis*, vol. 56, no. 3, pp. 191–252, 1974.

[24] R. Siegel, *Thermal Radiation Heat Transfer*, CRC press, 2001.

[25] A. Hussanan, I. Khan, and S. Shafie, "An exact analysis of heat and mass transfer past a vertical plate with Newtonian heating," *Journal of Applied Mathematics*, vol. 2013, 9 pages, 2013.

[26] K. J. Hollenbeck, "INVLAP. M: A Matlab function for numerical inversion of Laplace transforms by the De Hoog algorithm," 1998, http://www.isva.dtu.dk/staff/karl/invlap.htm.

[27] F. R. De Hoog, J. H. Knight, and A. N. Stokes, "An improved method for numerical inversion of Laplace transforms," *SIAM Journal on Scientific and Statistical Computing*, vol. 3, no. 3, pp. 357–366, 1982.

[28] M. Ali and M. Awais, "Laplace transform method for unsteady thin film flow of a second grade fluid through a porous medium," *Journal of Modern Physics*, vol. 5, no. 3, pp. 103–106, 2014.